Available online at www.sciencedirect.com

ScienceDirect

Procedia Engineering 139 (2016) 140 – 146

Procedia Engineering

www.elsevier.com/locate/procedia

MRS Singapore – ICMAT Symposia Proceedings

8th International Conference on Materials for Advanced Technologies

The Effects of Molecular Weight of a New Hole Transporting Polymer on the Organic Solar Cells Performance

Li Xianqiang[a,b], Li Jun[b], Wang Hong[a], Wu Dan[a], Tang Xiaohong[a]*

[a]*School of Electrical and Electronics Engineering, Nanyang Technological University, 50 Nanyang Avenue, Singapore 639798, Singapore*
[b]*Institute of Materials Research and Engineering (IMRE), Agency for Science, Technology and Research (A*STAR), 3 Research Link, Singapore 117602, Singapore*

Abstract

In this research, OSCs based on a new hole transporting polymer were fabricated. The highest power conversion efficiency of the device was received of 6.7% with the optimized molecular weight of the polymer. The charge carrier mobility in the OSCs was measured by using photoinduced charge extraction by linearly increasing voltage (PhotoCELIV) and time-of-flight (TOF) techniques. It is found that the charge carrier mobility is similar in the devices with both high and low molecular weight polymers. Light intensity dependence of the current-voltage characteristics was measured, which indicates strong bimolecular recombination in the low molecular weight polymer devices. Furthermore, the series and bulk resistances of the OSCs were obtained from the impedance measurement of the device. The high molecular device has a lower bulk resistance which corresponds to the weak bimolecular recombination of the device.

Selection and/or peer-review under responsibility of the scientific committee of Symposium 2015 ICMAT

Keywords: Organic solar cells; Molecular weight; Bimolecular recombination

1. Introduction

Harvesting solar energy is one of the most effective ways to tackle the energy shortage in the future. Organic photovoltaic (OPV) technology has been considered as a promising candidate of today's dominant PV technology

* Corresponding author. Tel.: +65-6790-4438; fax: +65-6790-4438.
E-mail address: exhtang@ntu.edu.sg

Selection and/or peer-review under responsibility of the scientific committee of Symposium 2015 ICMAT
doi:10.1016/j.proeng.2015.08.1121

based on inorganic materials. High material and manufacturing costs are problems for PV technology based on inorganic materials and limit its wide acceptance. Compared with inorganic PV materials, organic PV materials are much cheaper and can be easily processed. Organic solar cells (OSCs) also have other advantages, such as mechanical flexibility and light weight [1-4].

Thermal annealing and solvent annealing which are the most popular methods used to control morphology currently have been shown to tune the morphology of OSCs since 2005 [5, 6]. Poly(3-hexylthiphene) (P3HT) [7] is the most popular donor material and has been thoroughly studied in the last decade. For P3HT and PCBM system, thermal annealing method was found to significantly enhance J_{sc} and FF while V_{oc} slightly reduced upon thermal annealing. External quantum efficiency (EQE) of OSC based on P3HT can be increased after thermal annealing. This phenomenon is explained by enhancement of charge carrier transport as a result of increased hole mobility [8], improved morphology [9], and reduced recombination kinetics [10]. Detailed study of morphology change during thermal annealing reveals that fibrillar-like P3HT crystals which facilitate exciton separation and charge carriers transporting can be formed in PCBM crystals and amorphous P3HT. Solvent annealing approach, also called slow growth, is to store the film which stands in liquid phase in a confined petri dish after spin coating. A study on effects of solvent annealing method reveals that the benefits of solvent annealing, including recovering ordered structure, are more pronounced when PCBM loadings are higher [11]. Besides, some other approaches are also employed to tune the morphology, such as, optimization of weight ratio between polymer and fullerene and the concentration of solution, selection and mixture of solvents [12], and use of additives [13]. Molecular weight of polymers can also influence the morphology and performance of OSCs [14]. It has been reported that polymers with high molecular weight have ability to form smaller donor and acceptor domains because they have low solubility in solvent and will form polymer fibrillar networks which define smaller donor and acceptor domains while fullerene is still solubilized during the spin casting process. But so far, a comprehensive understanding of the effects of molecular weight on solar cells' performance is still missing.

In this paper, the effects of molecular weight of a new donor material on OSCs' performance are investigated. In this research, the charge carrier transporting properties and recombination mechanisms in OSCs based on polymers with different molecular weight are investigated. OSCs based on a new hole transporting polymer were fabricated. The highest power conversion efficiency of the device was received of 6.7% with the optimized molecular weight of the polymer. The charge carrier mobility in the OSCs was measured by using photoinduced charge extraction by linearly increasing voltage (PhotoCELIV) and time-of-flight (TOF) techniques. It is found that the charge carrier mobility is similar in the devices with both high and low molecular weight polymers. Light intensity dependence of the current-voltage characteristics was measured, which indicates strong monomolecular recombination in the low molecular weight polymer devices. The stronger bimolecular recombination in the lower weight polymer based solar cell is the main reason to lead to the lower PCE of the device. Furthermore, the series and bulk resistances of the OSCs were obtained from the impedance measurement of the device. The high molecular device has a lower bulk resistance which corresponds to the weak bimolecular recombination of the device. It is concluded that the different performance of the different molecular weight polymer devices can be attributed to the different bimolecular recombination of the carriers in the devices.

2. Experiment

The OSCs have a structure of ITO/PEDOT:PSS/Polymer:$PC_{71}BM$/Al. Polymer:$PC_{71}BM$ blend film were prepared from dichlorobenzene (DCB). The blend solution was stirred overnight at 45 ℃ in a glove box before spin casting.

ITO substrates were cleaned using soap water and sonicating sequentially with de-ionized water, acetone and isopropanol for 15 min each. The ITO substrates were dried at 100 ℃ in oven for several hours, followed by exposure to ultraviolet light and ozone for 15 mins to produce a hydrophilic surface. The cleaned ITO substrates were then transferred into a nitrogen-filled glove box. The PEDOT:PSS interlayers were spin-coated on the surface of ITO substrate followed by drying of the films at 140 ℃ for 10 min in ambient environment. Polymer:$PC_{71}BM$

blend film was spin-coated after heating the solution and ITO substrates at 100 ℃ for 10 min then annealed at 100 ℃ for 10 min to form an active layer. Different active layer thicknesses were achieved by varying the solution concentration and spin speed. A 100 nm Al layer was deposited by thermal evaporation at a base pressure of 1.0×10^{-6} mbar to form the cathode. The device area was defined to be 9.0 mm^2.

The thickness of active layer was measured by a KLA Tencor P-16+ Surface Profiler. The absorption spectrum of pure polymer and polymer:$PC_{71}BM$ blend films coated on quartz substrates were characterized by a Shimadzu UV-3101PC UV-VIS-NIR Spectrophotometer. The Nanowizard III instrument (JPK Instruments AG, Berlin, Germany) equipped with the NanoWizard head and controller was used in the AFM measurement. The morphology of the model surfaces was visualized by tapping mode AFM imaging under ambient conditions using standard silicon probes (k ~ 40 N/m, Tap 300AL-G, Budget sensors). All the images were processed using the JPK data processing software (Version 4.2).

PhotoCELIV setup is consisted of a pulsed Nd:YAG laser, pulse generator, function generator and a digital oscilloscope. The device with active layer which has an optimized thickness of 100 nm was excited by the laser with pulse width and pulse energy being about 4 ns and 17 mJ/cm^2. The laser wavelength was set at 640 nm and the laser pulse excited the device through the ITO side. The excited carriers were extracted by a linearly increasing voltage pulse. Offset voltage which approached to Voc was applied to compensate the build-in field. The TOF measurement was conducted on thick films with thickness more than 300 nm to ensure all carriers were generated on ITO side. The samples for TOF measurement have a simple structure which is ITO/polymer:$PC_{71}BM$/Al. The parameters of laser are the same as that used in photoCELIV measurement. In TOF measurement, the laser intensity needs to be adjusted to avoid space charge effects. The details of photoCELIV and TOF setup can be found somewhere else [15, 16].

3. Results and analysis

Fig. 1 shows the chemical structure of the new polymer and $PC_{71}BM$ and the schematic structure of OSCs. The device structure is a normal structure which means that transparent ITO acts as anode. PEDOT:PSS is inserted between Polymer:$PC_{71}BM$ blend as HTL.

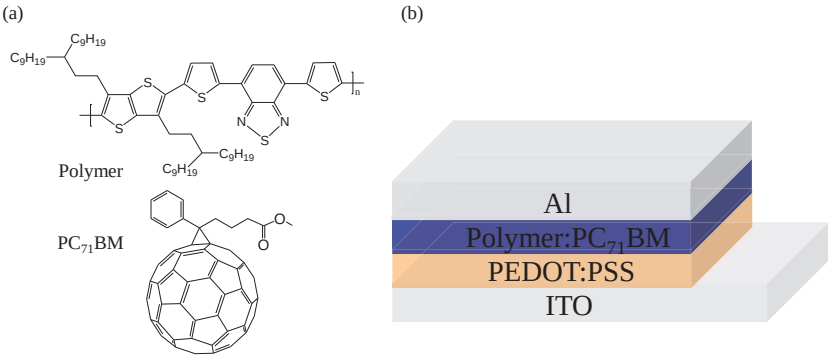

Fig. 1. (a) Chemical structure of materials used in this study. (b) schematic structure of OSCs.

Number-average molecular weight (M_n) is shown in Table 1 which also includes the photovoltaic parameters of OSCs based on polymer:$PC_{71}BM$. Two batches of polymers with different M_n were used to fabricate OSCs. All OSCs for polymers in each batch were optimized independently. The optimized weight ratio of polymer (19.0 kDa) and $PC_{71}BM$ is 1:1. For polymer with M_n = 49.5 kDa, the optimized weight ratio is 1:1.5. The highest PCE of polymer with high M_n is 6.71% which is much higher than that of polymer with low M_n, which is only 4.88%. From Table 1, it can be clearly seen that high M_n polymer has better performance because of a higher J_{sc}, 15.65 mA/cm^2, than that of low M_n polymer which is 11.24 mA/cm^2.

Table 1. Photovoltaic parameters of OSCs based on 19.0 kDa and 49.5 kDa polymers.

M_n (kDa)	Weight ratio (D/A)	J_{sc}(mA/cm^2)	V_{oc}(V)	FF(%)	PCE (%)
19.0	1:0.8	9.29	0.65	48.76	3.00
	1:1	11.24	0.72	60.40	4.87
	1:1.2	12.54	0.67	56.40	4.74
49.5	1:1.2	13.63	0.69	61.86	5.86
	1:1.5	15.65	0.70	61.31	6.76
	1:1.8	13.22	0.76	62.68	6.30

As mentioned before, J_{sc} is can be increased by narrowing bandgap of polymer as a result of absorbing more incident photons but in our experiment different J_{sc} is not due to bandgap because both absorption spectra have similar absorption peaks. Besides bandgap, charge carrier mobility can also influence J_{sc}. Charge carrier mobility can be affected by morphology, field, recombination or carrier densities under operation conditions. To get reliable results, PhotoCELIV measurement was conducted on the optimized devices to measure charge carrier mobility. The charge carrier mobility of low M_n OSCs ranges from 1.90×10^{-4} $cm^2V^{-1}s^{-1}$ to 1.15×10^{-4} $cm^2V^{-1}s^{-1}$ as electric field decreases. The charge carrier mobility of high M_n OSCs ranges from 2.49×10^{-4} $cm^2V^{-1}s^{-1}$ to 1.12×10^{-4} $cm^2V^{-1}s^{-1}$. Since the charge carriers in both systems have similar values, the different device performance is not caused by other factors rather than charge carrier mobility.

Unbalanced hole and electron transport can lead to accumulation of the slower carriers within the device and the photocurrent is space-charge limited then governed by a square-root dependence on bias. To study whether J_{sc} is limited by unbalanced hole and electron transports in low M_n OSCs, TOF technique was used to measure hole and electron mobility respectively in both systems. The carrier mobility of high M_n OSCs calculated in TOF measurement is slightly lower than that of low M_n OSCs which is different from the result of photoCELIV measurement. It might be attributed to morphology change in thick film which is necessary for TOF measurement. The absolute values of carrier mobility are not important since we want to investigate whether the hole and electron transports are balanced. Hole mobility, μ_h, and electron mobility, μ_e, of low M_n OSC are 1.81×10^{-4} $cm^2V^{-1}s^{-1}$ and 1.37×10^{-4} $cm^2V^{-1}s^{-1}$ when the sqrt of strength of electrical field is around $500\ V^{1/2}/cm^{1/2}$. The ratio between hole and electron mobilities is $\mu_h/\mu_e = 1.32$. In high M_n OSC, μ_h and μ_e are 1.09×10^{-4} $cm^2V^{-1}s^{-1}$ and 6.52×10^{-5} $cm^2V^{-1}s^{-1}$ and $\mu_h/\mu_e = 1.67$. In both high and low M_n systems, the hole and electron transports are balanced because the ratios between hole and electron mobilities are close to unity so the low J_{sc} in low M_n OSC is not limited by unbalanced hole and electron transport.

From photoCELIV and TOF measurements, it is found that the charge carrier mobility is not influenced by M_n and hole and electron transports are well balanced in both high and low M_n systems. In this case, different recombination mechanisms might be the reason why low M_n OSCs have poor performance. To study the recombination mechanisms, a simple technique of light intensity dependence of J-V characteristics is used. The J-V characteristics of OSCs based on different M_n polymers for the illumination intensity ranging from 100 mW/cm^2 to 0.1 mW/cm^2 are shown in Fig. 2 (a) and (c). Total current density (J_{total}) in OSCs can be expressed as a combination of dark diode current density (J_{dark}) and photogenerated current density (J_{ph}). $P_c(I,V)$ is the charge collection probability [17]. P_c-V characteristics under different illumination intensity are shown in Fig 2 (b) and (d). From saturation point to the maximum power point (MPP), the internal field is strong enough to sweep out carriers to

electrodes. Some authors have reported that monomolecular recombination is the dominant recombination mechanism in this range in their systems [18, 19]. Their conclusions are based on the phenomenon that P_c is independent of illumination light intensity from saturation point to MPP and $J_{ph, sat}$ is proportional to light intensity. Beyond MPP, the internal electric field is compensated by applied bias thus carriers cannot be efficiently swept out due to a lack of driving force from internal field. As a result, the recombination mechanism evolves from monomolecular recombination to bimolecular recombination. Different from their findings, in our experiment the bimolecular recombination dominates from saturation point -0.5 V to 1.0 V in low M_n OSCs as shown in Fig 2 (b) because even at small negative revers bias a large spread of P_c curves can be observed. In contrast, only a small spread of P_c curves is observed in the high M_n OSC which means bimolecular recombination is more severe in the low M_n OSC. Moreover, FF of the high M_n OSC remains unchanged as reducing illumination light intensity while FF of the low M_n OSC decreases from about 60% to less than 35% as light intensity decreases from 100 mW/cm^2 to 0.1 mW/cm^2. These results indicate that bimolecular recombination is not the dominant recombination in the high M_n OSC while in the low M_n OSC bimolecular recombination has a significant contribution to carriers loss. The different recombination mechanism in the OSCs with different M_n might be the reason that high M_n OSCs have better performance.

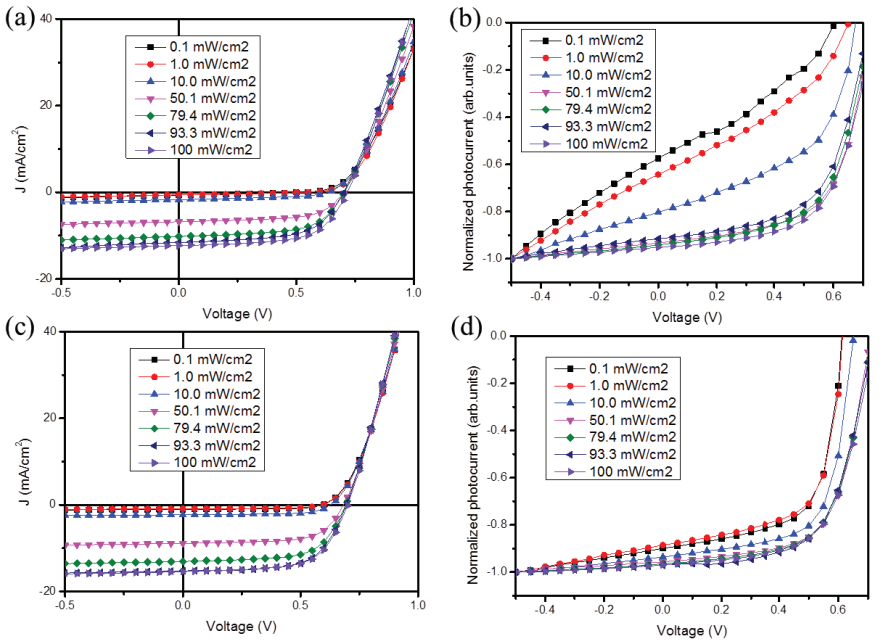

Fig. 2. J-V characteristics (a,c) and the charge collection probability (b,d) of OSCs with M_n 19.0 kDa and 49.5 kDa respectively.

To further understand the influence of M_n on device performance, the series and bulk resistance of OSCs were measured by impedance analysis under V_{oc} and 1 sun conditions. The Nyquist plots of OSCs using different M_n polymers are shown in Fig 3. The high M_n OSC has much lower bulk resistance indicated by the smaller radius of Nyquist plot [20]. Series resistance of the devices can be obtained by extrapolating the impedance curves to x-axis at low frequency (left). The series resistances of high M_n and low M_n OSCs are 2.1 Ωcm^2 and 1.9 Ωcm^2 respectively. The lower bulk resistance of the high M_n OSC might be a result of weak bimolecular recombination in the active layer, but due to the rough surface of active layer the series resistance of the high M_n OSC is higher than that of the low M_n OSC. The impedance analysis results are in agreement with the light intensity dependence of P_c-V characteristics experiment.

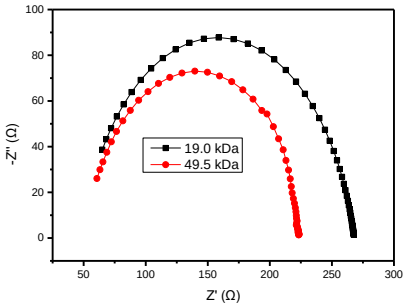

Figure 3. Nyquist plots of the impedance of polymer:$PC_{71}BM$ solar cells based on different M_n polymers.

4. Conclusion

In summary, two OSCs based on different M_n polymers were fabricated and optimized. The high M_n OSC has better performance than the low M_n OSC. The highest PCE is 6.7% and occurs when using high M_n polymer as donor. Low J_{sc} of the low M_n OSC limits its PCE. PhotoCELIV and TOF techniques were used to study the charge carrier mobilities in the two OSCs. It is found that in both OSCs the charge carrier mobilities are close and electron and hole transports are well balanced. Light intensity dependence of J-V characteristics of the two OSCs shows that bimolecular recombination is more severe in the low M_n OSC. The severe bimolecular recombination in the low M_n OSC limits its J_{sc} thus it has poor device performance. From impedance analysis, it is found that the high M_n OSC has lower bulk resistance and higher series resistance than the low M_n OSC which are in agreement with the light intensity dependence of J-V characteristics. These results indicate that high M_n can improve OSCs' performance by suppressing bimolecular recombination within the active layer. M_n is an important parameter for OSCs and should be considered when designing highly efficient OSCs.

Acknowledgements

The authors are grateful for finical support from A*STAR IMRE Printable High Performance Semiconducting Materials for OPVs and OTFTs Project (IMRE/11-2C0213). One of the authors, Li Xianqiang, also thanks NTU for NTU Research Scholarship.

References

[1] S.H. Park, A. Roy, S. Beaupre, S. Cho, N. Coates, J.S. Moon, D. Moses, M. Leclerc, K. Lee, A.J. Heeger, Bulk heterojunction solar cells with internal quantum efficiency approaching 100&percnt, Nature photonics, 3 (2009) 297-302.

[2] H.-Y. Chen, J. Hou, S. Zhang, Y. Liang, G. Yang, Y. Yang, L. Yu, Y. Wu, G. Li, Polymer solar cells with enhanced open-circuit voltage and efficiency, Nature Photonics, 3 (2009) 649-653.

[3] Y. Liang, Z. Xu, J. Xia, S.T. Tsai, Y. Wu, G. Li, C. Ray, L. Yu, For the bright future—bulk heterojunction polymer solar cells with power conversion efficiency of 7.4%, Advanced Materials, 22 (2010) E135-E138.

[4] J.H. Seo, A. Gutacker, Y. Sun, H. Wu, F. Huang, Y. Cao, U. Scherf, A.J. Heeger, G.C. Bazan, Improved high-efficiency organic solar cells via incorporation of a conjugated polyelectrolyte interlayer, Journal of the American Chemical Society, 133 (2011) 8416-8419.

[5] G. Li, V. Shrotriya, J. Huang, Y. Yao, T. Moriarty, K. Emery, Y. Yang, High-efficiency solution processable polymer photovoltaic cells by self-organization of polymer blends, Nature materials, 4 (2005) 864-868.

[6] W. Ma, C. Yang, X. Gong, K. Lee, A.J. Heeger, Thermally stable, efficient polymer solar cells with nanoscale control of the interpenetrating network morphology, Advanced Functional Materials, 15 (2005) 1617-1622

[7] F. Padinger, R.S. Rittberger, N.S. Sariciftci, Effects of postproduction treatment on plastic solar cells, Advanced Functional Materials, 13 (2003) 85-88.
[8] T.J. Savenije, J.E. Kroeze, X. Yang, J. Loos, The effect of thermal treatment on the morphology and charge carrier dynamics in a polythiophene–fullerene bulk heterojunction, Advanced Functional Materials, 15 (2005) 1260-1266.
[9] X. Yang, J. Loos, S.C. Veenstra, W.J. Verhees, M.M. Wienk, J.M. Kroon, M.A. Michels, R.A. Janssen, Nanoscale morphology of high-performance polymer solar cells, Nano letters, 5 (2005) 579-583.
[10] A. Pivrikas, G. Juška, A.J. Mozer, M. Scharber, K. Arlauskas, N. Sariciftci, H. Stubb, R. Österbacka, Bimolecular recombination coefficient as a sensitive testing parameter for low-mobility solar-cell materials, Physical review letters, 94 (2005) 176806.
[11] G. Li, Y. Yao, H. Yang, V. Shrotriya, G. Yang, Y. Yang, " Solvent annealing" effect in polymer solar cells based on poly (3-hexylthiophene) and methanofullerenes, Advanced Functional Materials, 17 (2007) 1636.
[12] S.E. Shaheen, C.J. Brabec, N.S. Sariciftci, F. Padinger, T. Fromherz, J.C. Hummelen, 2.5% efficient organic plastic solar cells, Applied Physics Letters, 78 (2001) 841-843.
[13] J. Peet, J.Y. Kim, N.E. Coates, W.L. Ma, D. Moses, A.J. Heeger, G.C. Bazan, Efficiency enhancement in low-bandgap polymer solar cells by processing with alkane dithiols, Nature materials, 6 (2007) 497-500.
[14] J.A. Bartelt, J.D. Douglas, W.R. Mateker, A.E. Labban, C.J. Tassone, M.F. Toney, J.M. Fréchet, P.M. Beaujuge, M.D. McGehee, Controlling Solution‐Phase Polymer Aggregation with Molecular Weight and Solvent Additives to Optimize Polymer‐Fullerene Bulk Heterojunction Solar Cells, Advanced Energy Materials, 4 (2014).
[15] R.A. Klenkler, G. Xu, H. Aziz, Z.D. Popovic, Charge-carrier mobility in an organic semiconductor thin film measured by photoinduced electroluminescence, Applied physics letters, 88 (2006) 242101.
[16] S. Shekhar, P. Ryberg, J.F. Hartwig, J.S. Mathew, D.G. Blackmond, E.R. Strieter, S.L. Buchwald, Reevaluation of the mechanism of the amination of aryl halides catalyzed by BINAP-ligated palladium complexes, Journal of the American Chemical Society, 128 (2006) 3584-3591.
[17] S.R. Cowan, R. Street, S. Cho, A. Heeger, Transient photoconductivity in polymer bulk heterojunction solar cells: competition between sweep-out and recombination, Physical Review B, 83 (2011) 035205.
[18] S.R. Cowan, A. Roy, A.J. Heeger, Recombination in polymer-fullerene bulk heterojunction solar cells, Physical Review B, 82 (2010) 245207.
[19] A.K.K. Kyaw, D.H. Wang, V. Gupta, W.L. Leong, L. Ke, G.C. Bazan, A.J. Heeger, Intensity dependence of current–voltage characteristics and recombination in high-efficiency solution-processed small-molecule solar cells, ACS nano, 7 (2013) 4569-4577.
[20] H. Zhou, Y. Zhang, J. Seifter, S.D. Collins, C. Luo, G.C. Bazan, T.Q. Nguyen, A.J. Heeger, High‐Efficiency Polymer Solar Cells Enhanced by Solvent Treatment, Advanced Materials, 25 (2013) 1646-1652.